RF BREAKDOWN IN X-BAND WAVEGUIDES*

Valery A. Dolgashev, Sami G. Tantawi†, SLAC, Stanford, CA 94309, USA

1 INTRODUCTION

Next generation of linear accelerators will have multi-megawatt rf systems. The RF system of the Next-Linear Collider (NLC) will have hundreds of waveguide components and high-gradient accelerating structures. Waveguide components should reliably handle up to 600 MW of a 400 ns, 11.424 GHz rf pulse [1]. RF breakdown at such high power could damage these components. For example, breakdown damage is a major issue for long term operation of high-gradient accelerating structures [2]. An extensive experimental and theoretical program to study phenomena of rf breakdown is under way in SLAC. This work is a part of this program. Our experiments with rf breakdowns in a copper low-magnetic field waveguide are described in [3]. Here we discuss study of a copper high-magnetic-field waveguide and a low-magnetic-field waveguide with walls made of copper, gold and stainless steel. All experiments are done at a frequency of 11.424 GHz.

1.1 RF breakdown and experimental conditions

We define rf breakdown as a phenomenon that abruptly and significantly changes transmission and reflection of the rf power directed to the structure under test. Breakdown is accompanied by a burst of x-rays and by a bright flash of visible light. Initiation of an rf breakdown process and the dynamics of its development are greatly effected by the geometry of the structure under test, by the rf energy available for the breakdown, and by the external circuit. For example, the amplitude of the breakdown electric field varies from 600 MV/m at 200 ns pulse width for a small cavity (L. Laurent [4]) to about 200 MV/m at 240 ns in traveling wave accelerating structures (C. Adolphsen, [5]). Because of this variation, we have chosen operating conditions for the waveguide test close to those of high power waveguides and traveling wave accelerating structures: rf power $\sim$ 100 MW; area of high electric field $\sim$10 cm^2; rf pulse width $\sim$ 1 μs; energy absorbed in a breakdown $\sim$ 10 J; gap between high electric field surfaces $\sim$1 cm.

1.2 Magnetic field

To determine the effect of different geometries on properties of rf breakdown we designed geometries of two rectangular waveguides. We kept such parameters as high-electric-field surface area and peak electric field for given input power (80 MV/m for 100 MW) the same for both waveguides. The major differences are the topology and the magnitude of rf magnetic field. At 100 MW rf power, at region of maximum surface electric field the magnetic field is 0.04 MA/m in low-magnetic-field waveguide and 0.17 MA/m in high magnetic field waveguide. Thanks to the simplicity of the waveguede geometry, it was easy to use semi-analytical and 3D Particle-In-Cell codes for simulation of the breakdown dynamics.

1.3 Materials

To study the effect of different materials on breakdown behaviour we have tested gold and stainless steel waveguides together with copper waveguide. Gold was chosen to evaluate possible effects of heavier ions (atomic weight of gold 197 *vs.* 63.3 copper) on breakdown thresholds. We have used stainless steel A304 for the other waveguide. This steel is widely used for vacuum components such as vacuum flanges.

1.4 Initial contamination

We believe that large rf energy available for the breakdown (up to 100 J) significantly reduces the uncertainty of initial surface contamination. This assumption was supported by inspection of the surfaces of the waveguides after processing. This inspection has shown that the surfaces are drastically modified from their initial condition.

2 WAVEGUIDES OF DIFFERENT GEOMETRIES

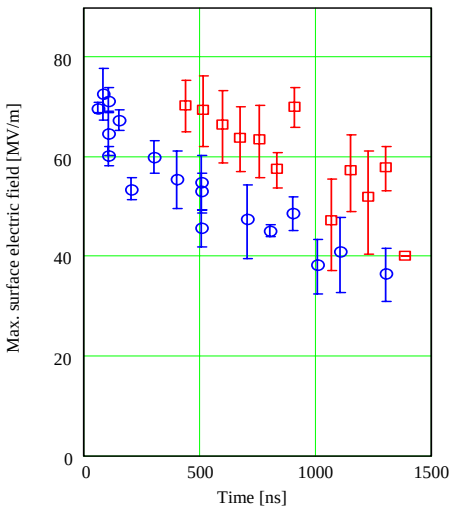

Figure 1: Maximum surface electric field *vs.* pulse length for waveguides with different geometries: circles - high magnetic field waveguide, boxes - low magnetic field waveguide.

The width of the low-magnetic-filed waveguide was reduced to 1.33 cm (in comparison with a width of 2.29 cm

* This work was supported by the U.S. Department of Energy contract DE-AC03-76SF00515.

† Also with the Communications and Electronics Department, Cairo University, Giza, Egypt.

for WR90) over a length of 8.71 cm in order to enhance the electric field by lowering the group velocity to 0.18c, and force the breakdown to occur in this area. The width of the high-magnetic-filed waveguide was the same as WR90. To increase electric field, the height was reduced to 1.27 mm (from $\sim$1 cm of WR90) over a length of 5.1 cm. Group velocity in this last waveguide is 0.82c. We subjected the waveguide to rf power up to 120 MW with pulse widths up to 1.4 μs. We performed the following procedure: pulse width was set to a certain value then power was ramped up until rf power was switched off by the klystron control system. The control system is monitoring vacuum inside the waveguide. Burst of gas generated by the breakdowns triggered the control system. We recorded the incident, transmitted and reflected rf power for every pulse; the intensity of light emission and its spectrum; the intensity of X-rays; and harmonics of the working frequency of 11.424 GHz. Harmonics were present in the klystron output as well as being generated by rf breakdown. Dependence of mean value of rf power with it's standard deviation *vs.* pulse length is shown on Fig. 1. During testing pulse length was changed randomly. Data obtained during first hours of processing is excluded from this graph. Data for low-magnetic-field waveguide and pulse length shorter than 400 ns is not shown because maximum electric field was limited not by the breakdowns but by available rf power. We list some similarities in breakdown behavior deduced from the results of this experiment:

1. Transmitted power has a repeatable shape: it drops off to zero with an amplitude proportional to $e^{\frac{-(t-t_s)^2}{2\tau^2}}$ (Gaussian-like). Here t_s is breakdown start time. The rf pulse starts at $t = 0$.
2. Transmission does not recover for several microseconds after the breakdown.
3. Up to 90% of the incident rf energy is absorbed after $t_s + 2\tau$.
4. RF transmission fully recovers after the main rf pulse has been off for several milliseconds.
5. Light (emitted from the breakdown site) lasts for several microseconds after the rf pulse.
6. Spectral lines of the light are mostly from neutral copper atoms (Cu I).
7. In most events, the 3rd harmonic (34.272 GHz) signal from the klystron transmitted through the breakdown site is shut off by the breakdown.
8. Breakdown produces a 3rd harmonic of the klystron signal, and, probably, higher harmonics.
9. Characteristic size of the damaged spots on the surface of the waveguide is $\sim$ 10–100 μm. Some traces have size of $\sim$1 mm.

Here we list differences in breakdown behavior for the waveguides:

1. Breakdown electric fields are higher for low-magnetic-field waveguide by about 30%.
2. Most of breakdowns in low-magnetic-field waveguide have a drop off time constant τ between 20 and 200 ns. For high-magnetic-field waveguide τ has a value between 10 and 50 ns.
3. Metal surface is damaged more in high-magnetic-field waveguide. Surface damage on low-magnetic-field waveguide had a depth of a few μm; in the other waveguide this depth is in the order of 100 μm.
4. Deviation of maximum amplitudes of the breakdown fields at chosen pulse width is larger for low-magnetic-field waveguide (see Fig. 1).
5. We monitored vacuum pressure by measuring currents of vacuum pumps. Gas released by a few consequent breakdowns (or even a single breakdown) in low-magnetic-field waveguide increases the current by several orders of magnitude. This increase forces the automatic control system to switch off rf power. The amount of gas generated by breakdowns in high-magnetic-field waveguide was much smaller than in low-magnetic-filed waveguide. We observed thousands consecutive breakdowns (at repetition rate up to 60 Hz) in this waveguide with minor change in the pump's current.
6. In low-magnetic-field waveguide, breakdowns at rf high power ($\sim$ 100MW) and short pulse length ($\sim$ 300 ns) and breakdowns at longer pulse length had decreased dark currents. Lower power and a longer pulse (more than 400 ns) increases dark currents. We think that the level of dark currents indicates the degree of metal surface damage. With high magnetic-field-waveguide we did not observe such phenomenon.

We tested the effect of low temperature on breakdown threshold for both waveguides. We cooled the waveguides by boiling liquid nitrogen in a bath that surrounded the waveguides for $\sim$2 hours. We didn't observe any change in the level of breakdown fields due to low temperature.

2.1 Simulations

We have used the commercial Particle-In-Cell (PIC) code MAGIC [6] for simulation of the breakdown dynamics in both waveguides. We describe the model and results for low-magnetic-filed waveguide in [3]. The main difference in breakdown dynamics between the waveguides is the time that copper ions fill the waveguide gap. This time is about one third as long ($\sim$ 10 ns vs. $\sim$ 30 ns) for high-magnetic-field waveguide; the height of the waveguides is 8 times different. We think that this difference in ion fill time could explain observed small difference in drop off time constant τ.

3 DIFFERENT MATERIALS

We have followed the same testing procedure (as for copper low-magnetic-field waveguide) for two other waveguides of the same geometry: gold-plated and stainless steel waveguides.

3.1 Results

The general properties of breakdown behaviour (complete power shut off, up to 90% of power absorbed, burst of X-rays and visible light that lasts several microseconds)

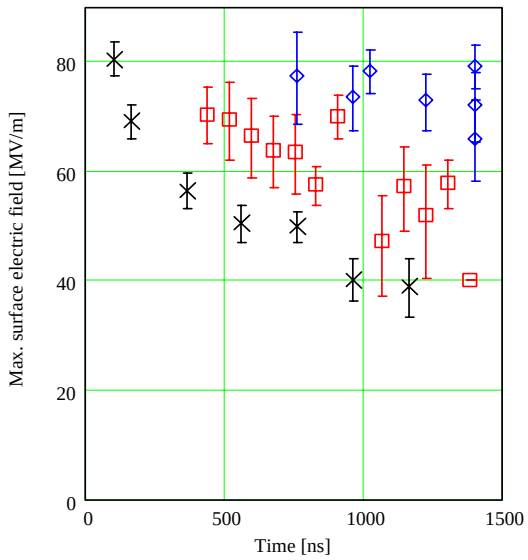

Figure 2: Maximum surface electric field *vs.* pulse length for low-magnetic-field waveguides with walls made of different materials: boxes - copper, x - gold plated, diamonds - stainless steel.

were very similar for all three materials. Traces of localized arcs on the metal surface had similar structure and size. We think that this similarity is an evidence that the basic physics of breakdown is independent of material. The level of breakdown fields was higher for stainless steel than for copper and lower for gold as shown in Fig.2. This difference was obvious from the first hours of processing. The graph does not show data for stainless steel waveguide for pulse width lower than 700 ns because we were limited by available klystron power and breakdowns in the klystron-to-test-setup waveguide system rather than by breakdowns in the steel waveguide itself. Breakdown electric field *vs.* pulse length characteristic of gold waveguide was very similar to that of high-magnetic field waveguide: mean values are lower and deviations are smaller than that of copper and steel waveguides.

4 DARK CURRENTS

All waveguides we have tested emitted X-rays during non-breakdown high power rf pulses. We monitored this radiation by photo-multiplier-tubes (PMT) with scintillators. We recorded the dependence of these signals on incident rf power. We fitted results to the Fowler-Nordheim equation, using PMT voltage instead of dark current. As a result of the fitting, we obtained amplification factor **B** of an X-ray signal. This **B** is not an exact equivalent of β in the Fowler-Nordheim equation. We will not discuss the relation between **B** and β in this paper. Here we list the results of these measurements:

1. During processing, **B** decreased by $\sim$10–20% while the amplitude of PMT signals dropped by anorder of magnitude.
2. A breakdown increased or decreased amplitude of PMT signal by 10–300% and change **B** by $\sim$10–20%.
3. Sources of X-rays are localized in the waveguide. Breakdowns change this localization.
4. Waveguides with higher breakdown thresholds have lower average **B**: high-magnetic-filed copper waveguide - 120; low-magnetic-field gold waveguide - 125; low-magnetic-field copper - 80; low-magnetic-field stainless steel - 47. Since the change of **B** during processing is small, it allows us to estimate breakdown thresholds for given waveguide without extensive processing.

5 SUMMARY

Comparison of two geometries shows that macroscopic geometry is very important in breakdown phenomena. High-magnetic-field waveguide has a lower breakdown threshold than low-magnetic-field waveguide. The electric field gap is much smaller (1.3 mm *vs.* 10 mm) in the high-magnetic-field waveguide. This gap dependence contradicts a DC model of the breakdown, where breakdown threshold decreases with increased gap.

Breakdown properties are also strongly dependent on surface material. Stainless steel waveguide we tested had a higher breakdown threshold than copper and gold, and gold had a lower threshold than copper. Stainless steel and copper have similar thermal expansion coefficients. This similarity makes practical manufacturing of copper-steel structures. Such structures could have better breakdown properties than copper-only structures. For instance, tips of irises in high gradient accelerating structures could be made of stainless steel.

X-rays initiated by dark currents may help to understand onset of breakdown and estimate breakdown thresholds without extensive processing.

6 REFERENCES

[1] "2001 Report on The Next Linear Collider," SLAC-PUB-R-571, Snowmass, Colorado, 2001.

[2] C. Adolphsen *at al*, "RF Processing of X-Band Accelerator Structures at the NLCTA," LINAC2000, August, 2000, Monterey, Ca.

[3] Valery A. Dolgashev, Sami G. Tantawi, "Simulations of Currents in X-band accelerator structures using 2D and 3D particle-in-cell code," FPAH057, Proceedings of the 2001 Particle Accelerator Conference, June 18-22, Chicago, Illinois. pp. 3807-3809.

[4] L.Laurent*at al*,"Pulsed RF Breakdown Studies, " SLAC-PUB-8409, March 2000.

[5] C. Adolphsen *at al*, ROAA003, Proceedings of PAC01, June 18-22, Chicago, Illinois. pp. 478-480.

[6] http://www.mrcwdc.com/Magic/